Building and Environment 224 (2022) 109535

Contents lists available at ScienceDirect

Building and Environment

journal homepage: www.elsevier.com/locate/buildenv

Aerogel composite for cavity wall rehabilitation in the Netherlands: Material characterization and thermal comfort assessment

C.H. Koh *, K. Schollbach, F. Gauvin, H.J.H. Brouwers

Department of the Built Environment, Eindhoven University of Technology, P. O. Box 513, 5600 MB, Eindhoven, the Netherlands

ARTICLE INFO

Keywords:
Aerogel composite
Thermal conductivity
Moisture
Hygrothermal performance
Occupant comfort

ABSTRACT

Energy retrofitting of existing building stocks is essential to reduce building-related energy consumption. Cavity wall insulations are commonly applied, however, their hygrothermal performance is not well established. This study focuses on the hygrothermal performance of rehabilitated cavity walls in the Netherlands. A state-of-the-art aerogel composite developed for cavity wall retrofitting using the blown-in method is presented. The aerogel composite has a dry thermal conductivity of 22.5 $mW{\cdot}m^{-1}{\cdot}K^{-1}$ and low sorption isotherms. A retrofitted masonry wall with a 6 cm cavity using the aerogel composite can achieve thermal transmittance (U-value) of 0.32 $W{\cdot}m^{-2}{\cdot}K^{-1}$, well below the 0.71 $W{\cdot}m^{-2}{\cdot}K^{-1}$ required in the Netherlands. It can reduce the annual heating and cooling demand by up to 72% in a simulated building, and also provides better thermal comfort to the occupants, lowering the percentage of thermally dissatisfied occupants from 51% to 18%. The tested aerogel composite outperforms conventional insulation materials in the market, without sacrificing the thermal comfort of its occupants.

1. Introduction

The building-related energy consumption in services and households sectors accounts for 37% of the total energy consumption in the Netherlands in 2020, and the largest part is being used for space heating [1]. To reduce greenhouse gas (GHG) emissions in the Netherlands, the Dutch government has committed to reducing CO_2 emissions in the building sector to net zero in 2050 [2]. To achieve this target, energy retrofitting of existing building stocks is indispensable.

Before the 1920s, single brick wall construction was commonly found in Dutch residential buildings, which often require a costly rehabilitation strategy [3]. However, in the mid-1920s, houses constructed with cavity walls began to appear in the Netherlands. By the late 1970s, requirements for thermal insulation were introduced in new buildings, and the cavity walls became wider and filled with better insulation material instead of air. It is those buildings with a cavity wall that were constructed in the period between the 1920s and 1970s, that can be filled in with insulation material without requiring major renovation. These building stocks account for approximately 40% of the total housing stock or equivalent to more than 3 million homes in the Netherlands, presenting a significant CO_2 emission reduction potential that is attainable. Just in 2020, over a million energy-saving measures were taken in existing housings in the Netherlands, and cavity wall insulation is one of the most commonly taken [1], with more than 3 million m^2 of cavity filling carried out by certified contractors [4].

A typical cavity filling procedure is drilling holes in the outside façade, and the insulation material is blown into the cavity through these holes. The holes will be grouted by the end of the filling [5]. In the Netherlands, the most commonly used blown-in insulation materials for cavity walls are glass wool, stone wool and expanded polystyrene (EPS) beads, followed by polyurethane (PU) foam, urea-formaldehyde (UF) foam and silicone-treated perlite. A brick wall with a 6 cm air cavity without any insulation material has a thermal transmittance (U-value) of around 2.50 $W{\cdot}m^{-2}{\cdot}K^{-1}$ and can reach 0.59 $W{\cdot}m^{-2}{\cdot}K^{-1}$ once new insulation material is filled in Ref. [5]. This improved U-value could satisfy the maximum U-value of 0.71 $W{\cdot}m^{-2}{\cdot}K^{-1}$ dictated for wall renovation in an existing building [6].

To further improve the U-value of retrofitted cavity walls using the blown-in insulation method, for example, to reach 0.21 $W{\cdot}m^{-2}{\cdot}K^{-1}$ required for a new building [7], an innovative, high-performance insulation product is essential. Superinsulation materials (with thermal conductivity values below 20 $mW{\cdot}m^{-1}{\cdot}K^{-1}$) are often applied, notably silica aerogel composites due to their low thermal conductivity, which can reach 12 $mW{\cdot}m^{-1}{\cdot}K^{-1}$ in their monolithic form, 15

* Corresponding author.
E-mail address: k.c.h.koh.chuen.hon@tue.nl (C.H. Koh).

https://doi.org/10.1016/j.buildenv.2022.109535
Received 14 June 2022; Received in revised form 23 August 2022; Accepted 24 August 2022
Available online 30 August 2022

$mW{\cdot}m^{-1}{\cdot}K^{-1}$ for an aerogel blanket, and 18 $mW{\cdot}m^{-1}{\cdot}K^{-1}$ in the granulate form [8].

Aerogel particles in the granulate form are presently commercialized as insulating cavity wall infill. A retrofitting example is a detached house in Biel Switzerland, where aerogel granulate was blown into the cavity walls with a 90 mm air gap, improving their U-value from 1.10 to 0.18 $W{\cdot}m^{-2}{\cdot}K^{-1}$ [9]. Other forms of blown-in aerogel insulation are being investigated. An aerogel product '*Spacefill*' was tested during the EFFESUS project [10], which is based on polyester fibre impregnated with aerogel, similar to an aerogel blanket. The composite was cut into 5 mm cubes and achieved thermal conductivity in the range of 18–25 $mW{\cdot}m^{-1}{\cdot}K^{-1}$ under both laboratory and mock-up testing [11,12]. Another state-of-the-art aerogel composite 'Airofill' has been developed for cavity wall retrofitting using the blown-in method. This product contains silica aerogel granulates, which are bound together with a propriety binder in a slurry form. Once the composite is blown into the cavity wall, it will solidify and subsequently dry up and form a continuous foam block inside. Other sprayable aerogel composites that can be used for cavity wall retrofitting offer thermal conductivity in the range of 20–27 $mW{\cdot}m^{-1}{\cdot}K^{-1}$ [13,14].

The original air gap in a cavity wall is designed to regulate moisture transport and to drain water in the cavity through air ventilation. It is, therefore, a concern that a filled cavity may give rise to inferior hygrothermal performance, and subsequently impact the thermal comfort of its occupants. To counter this concern, it is crucial to study the performance of blown-in insulation in a cavity wall under different environmental conditions. There is however a gap in the literature related to the hygrothermal performance after cavity wall rehabilitation, either using conventional blown-in insulation material or aerogel composite. The thermal conductivity of loose-fill blown-in stone wool, glass wool and cellulose can be compromised under humid conditions [15]; but there are some indications that aerogel composites (blanket [16–20] and render [21]) work well to protect the wall alleviate moisture risk owing to the hydrophobic nature of its main component silica aerogel. Case studies using aerogel composites (in the form of blankets and boards) for refurbishments of heritage buildings suggest an improvement in comfort level inside the buildings [9]. Studies also found that applying aerogel-based render on exterior walls can prevent condensation risk in existing buildings [22,23], however, the hygrothermal risk is predicted to increase in colder climates [23].

The hygrothermal performance of rehabilitated cavity walls has not been widely studied, and more investigations are required to examine the efficiency and their impacts on occupant thermal comfort conditions under a retrofitted building. This comparative study aimed to verify the performance of commercially available and state-of-the-art aerogel composite using the blown-in installation method. The thermal and hygric characteristics of the aerogel composite are examined and used to simulate the hygrothermal performance under a cavity wall construction and a typical Dutch climate, and conventional insulation materials are included for comparison purposes. Occupant thermal comfort conditions are further included to study the ergonomics of the thermal environment of a reference building using a simulation tool.

2. Material and methodology

The material properties and hygrothermal performance of the aerogel composite are evaluated using the methodology shown in Fig. 1. Thermal and hygric properties are measured in the laboratory, while validated software is used to model and simulate the performance of reference wall assembly and building consisting of the aerogel composite and the selected reference insulation materials under different boundary conditions.

2.1. Experimental characterisation

2.1.1. Material

The Airofill (hereafter referred to as the 'aerogel composite') is selected as the blown-in insulation material for cavity wall retrofitting. The aerogel composite was made by and supplied by Takkenkamp, Zelhem. The sample in foam block form is shown in Fig. 2a, which is mainly made up of hydrophobic silica aerogel granulates which are bound together with a proprietary organic binder and other additives for rheology modification and durability improvement. The composite is pre-mixed and kept in a slurry form in a tank prior to site operation. By using a blowing machine, the composite is blown into the cavity wall via an injection nozzle, and subsequently solidifies and dries up within the wall under an ambient environment to form a continuous brittle foam block inside. It should be noted that the binder is necessary to bind the aerogel granulates during and after the retrofitting process, to avoid the risk of aerogel granulates being dispersed into the surroundings (via leaking) where they could pose a potential health hazard to the occupants.

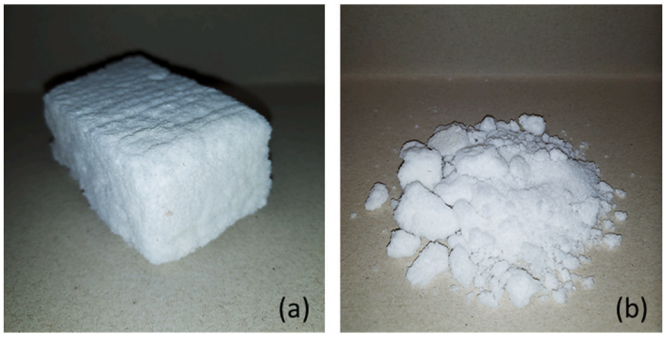

Fig. 2. Sample of the aerogel composite in (a) block form and (b) fragments.

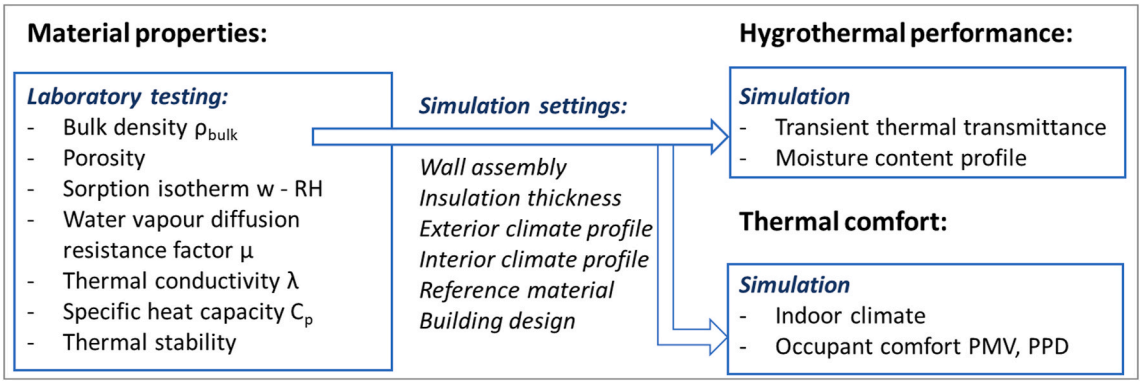

Fig. 1. Methodology overview.

2.1.2. Material properties characterization

The sorption isotherm of the aerogel composite is measured using the gravimetric sorption technique through dynamic vapour sorption (DSV) (Surface Measurement Systems DVS Resolution). The DVS apparatus has a declared accuracy of 0.5% (relative humidity reading) and a balance noise of less than 0.3 μg. Three sets of 12–15 mg fragmented samples are prepared. The samples are first dried in an oven at 70 °C until the constant mass is achieved to attain their dry weight m_{dry}. Using the DVS apparatus, the moisture content w of the specimen is measured from 0% up to 95% relative humidity RH for the sorption curve, and from 95% back to 0% RH for the desorption curve, with a constant temperature of 20 °C. The specimen is considered to reach its constant mass once the rate of mass change dw/dt (%kg·kg^{-1}·min^{-1}) is equal to or less than 0.01. The equilibrium moisture content w (%kg·kg^{-1}) is plotted against RH (%) for both sorption and desorption curves based on the median result.

Free water saturation w_{sat} is approximated by conditioning the specimen at 100% RH by means of fully immersing the specimen in water for 7 days at room temperature, an approximation method based on ASTM C1498-01 note 3 [24]. The surface of samples is then lightly blotted with a damp sponge to remove excess water and their weight is measured. Three sets of 40 × 40 × 35 mm samples are prepared, and the median result is taken to remove any outliers.

The water vapour diffusion resistance factor μ is measured using both the wet cup (distilled water) method and the dry cup (desiccant) method according to standard ASTM E96 [25]. The cups are filled with anhydrous calcium chloride $CaCl_2$ for the dry cup method and distilled water for the wet cup method. Specimen with a thickness d_μ (m) are attached to the cups with a specific exposed area A_μ (m^2) and the edges are sealed with aluminium tapes to block vapour passage at the edge of the specimen (Fig. 3). The test cups are kept in a climatized room at 60% RH and 20 °C. The change of mass Δm (kg) at successive times Δt (s) is measured by weighing the cups to obtain the density of water vapour transmission rate g (kg·m^{-2}·s^{-1}) as

$$g = \frac{1}{A_\mu}\frac{\Delta m}{\Delta t} \tag{1}$$

The measurement is considered complete once five successive values of g only vary within ±5%. The value of μ (dimensionless) is then calculated using

$$\mu = \frac{\Delta p \bullet \delta_{air}}{g \cdot d_\mu} \tag{2}$$

where Δp (Pa) is water vapour partial pressure difference and δ_{air} (kg·m^{-1}·s^{-1}·Pa^{-1}) is the water vapour permeability of air. One set of 40 × 40 × 35 mm sample is prepared for each cup.

The total porosity of the specimen (open and closed pores) is calculated from their particle density $\rho_{particle}$ (kg·m^{-3}) and bulk density ρ_{bulk} (kg·m^{-3}) as

$$porosity = 1 - \frac{\rho_{bulk}}{\rho_{particle}} \tag{3}$$

A helium pycnometer (Micromeritics AccuPyc II 1340) with a 10 cm^3 cup is used to measure their $\rho_{particle}$.

The steady-state thermal transmission test method is utilized for the measurement of thermal conductivity λ (W·m^{-1}·K^{-1}) by using a heat flow meter (Thermtest HFM-25), with a declared accuracy of 3% of the reading. The specimen is positioned between a pair of heating-cooling isothermal plate assemblies, with an upper-temperature setpoint at 30 °C and a lower setpoint at 10 °C, reaching an equilibrium mean temperature at 20 °C for the specimen. The steady-state heat flux generated due to the difference in temperature between the heating-cooling plates is used to measure the thermal resistance and calculate the thermal conductivity. Three sets of 40 × 40 × 20mm samples are prepared and conditioned separately under three RH (0%, 58% and 75%) for their λ values. The samples are dried at 70 °C in an oven (Memmert universal oven UF260) to reach near 0% RH and conditioned in a desiccator under aqueous solutions [24] for 58% RH (sodium bromide NaBr) and 75% RH (sodium chloride NaCl), all until constant weight is achieved. The samples are protected using low vapour permeability plastic wrap before and during the λ measurements to maintain their moisture content. The average measurement time for each specimen is around 1 h, potentially causing redistribution of the moisture in the sample, and resulting in an additional error in the measurement results. This limitation however is disregarded here and the moisture content is assumed to be constant throughout the specimen. In this study, the temperature dependence of the thermal conductivity is omitted and assumed to be constant within the simulated

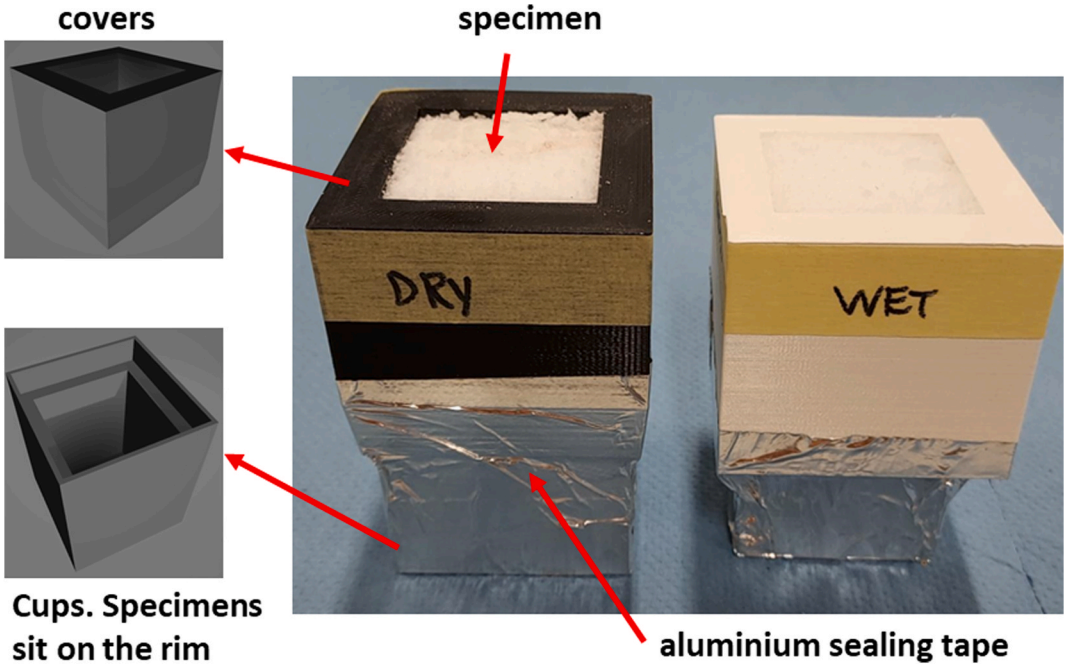

Fig. 3. The wet and dry cup method.

temperature range.

For specific heat capacity C_p ($J{\cdot}kg^{-1}{\cdot}°C^{-1}$), differential scanning calorimetry (TA Instruments DSC Q2000) is used at temperatures from −20 °C to 50 °C at a heating/cooling ramp of 10 °C·min^{-1} in a nitrogen atmosphere with a flow of 50 ml·min^{-1}. Three heat-cool cycles are run for the sample, and the C_p value at 20 °C from the third heat cycle is taken for the subsequent hygrothermal study. 3 mg of crushed sample is prepared.

Thermogravimetric analysis TGA (Netzsch Instruments STA F1 Jupiter Analyzer) is further used to investigate the thermal stability of samples from 40 °C up to 800 °C at a heating rate of 10 °C·min^{-1} in a nitrogen atmosphere with a flow of 20 ml·min^{-1} by observing their mass change due to thermal degradation.

2.2. Numerical simulation

2.2.1. Hygrothermal performances

Heat, air and moisture transport (HAM) simulations are performed for masonry wall assemblies with 6 cm cavity thickness exposed to the same climates. The annual moisture content of the insulation materials is analysed. A building with masonry cavity walls is further modelled to simulate the indoor climate for occupant comfort evaluation.

For the HAM simulations, one-dimensional non-steady heat and moisture transport processes are solved by the coupled differential equations using software WUFI Pro [26], i.e. heat transport and moisture transport by

$$\frac{\partial H}{\partial T}\frac{\partial T}{\partial t}=\frac{\partial}{\partial x}\left[\lambda\frac{\partial T}{\partial x}\right]+h_v\frac{\partial}{\partial x}\left[\frac{\delta}{\mu}\frac{\partial p}{\partial x}\right] \tag{4}$$

and

$$\rho_w\frac{\partial w}{\partial \varphi}\bullet\frac{\partial \varphi}{\partial t}=\frac{\partial}{\partial x}\left[\rho_w D_w\frac{\partial w}{\partial \varphi}\frac{\partial \varphi}{\partial x}\right]+\frac{\partial}{\partial x}\left[\frac{\delta}{\mu}\frac{\partial p}{\partial x}\right] \tag{5}$$

respectively, where D_w ($m^2{\cdot}s^{-1}$) is the liquid transport coefficient, H ($J{\cdot}m^{-3}$) the enthalpy, h_v ($J{\cdot}kg^{-1}$) the evaporation enthalpy of water, p (Pa) the water vapour partial pressure, w ($m^3{\cdot}m^{-3}$) the water content, δ ($kg{\cdot}m^{-1}{\cdot}s^{-1}{\cdot}Pa^{-1}$) the water vapour diffusion coefficient in air, T (°C) the temperature, λ ($W{\cdot}m^{-1}{\cdot}K^{-1}$) the thermal conductivity, μ (dimensionless) the vapour diffusion resistance factor, ρ_w ($kg{\cdot}m^{-3}$) the density of water, and φ (dimensionless) the relative humidity RH.

The left-hand side of both equations consists of the storage terms, while the transport terms are on the right-hand side. In this model, the heat storage consists of the heat capacity of the material, the heat transport includes both moisture-dependent thermal conductivity and vapour enthalpy flow, the moisture storage is directly linked to the sorption isotherm, and the moisture transport contains both the liquid transport and vapour diffusion terms.

The design of the assembly wall in this study is based on the common exterior wall found in older buildings in the Netherlands, i.e. masonry wall with a 6 cm thick air cavity, as shown in Fig. 4a-b. Glasswool, stone wool and PU foam are included in the HAM study as reference materials. For the masonry wall, 10 cm thick solid bricks are applied for both exterior and interior sides. Material properties of the referenced insulation materials and the masonry are listed in Table 1 and Fig. 5. The original cavity wall without insulation is modelled with an arbitrary air change rate of 10 h^{-1} (between the 5 and 20 h^{-1} used in Ref. [27]) in its cavity.

Eindhoven in the Netherlands is selected as the location for the hygrothermal analysis. Table 2 shows the annual weather summary, while Fig. 6 shows the annual air temperature and relative humidity profile [28]. The Netherlands experiences temperate oceanic climate Cfb type as per Köppen climate classification. The wall is facing the main driving rain direction (south-western) for the hygrothermal simulations in all cases. The interior climate is set as per EN 13788 to humidity class 3 which represents a building with unknown occupancy [29], and a constant air temperature of 20 °C. The simulation is run for ten years or until hygrothermal equilibrium is reached.

2.2.2. Indoor climate and occupant comfort assessment

The indoor climate and comfort conditions in a reference building with masonry cavity walls are further investigated using the software WUFI Plus, by calculating the balance of the heat and moisture transfers in the room [31], i.e. heat balance and moisture balance by

$$\frac{\partial H}{\partial t}=\sum_j Q_{comp,j}+Q_{sol}+Q_{in}+Q_{vent}+Q_{HVAC} \tag{6}$$

Table 1
Material properties for solid brick, glasswool, stone wool and PU foam for simulation [30].

	Solid Brick	Glasswool	PU Foam	Stone Wool
Bulk density ρ_{bulk}, dried ($kg{\cdot}m^{-3}$)	1900	36	39	60
Porosity (%)	0.24	0.986	0.99	0.95
Specific heat capacity C_p ($J{\cdot}kg^{-1}{\cdot}K^{-1}$)	850	850	1470	850
Thermal conductivity λ ($W{\cdot}m^{-1}{\cdot}K^{-1}$)	0.6	0.0343	0.025	0.04
Vapour diffusion resistance factor μ (dimensionless)	10	1.3	88.93	1.3
Free water saturation w_{sat} (%)	10	1017	72	75

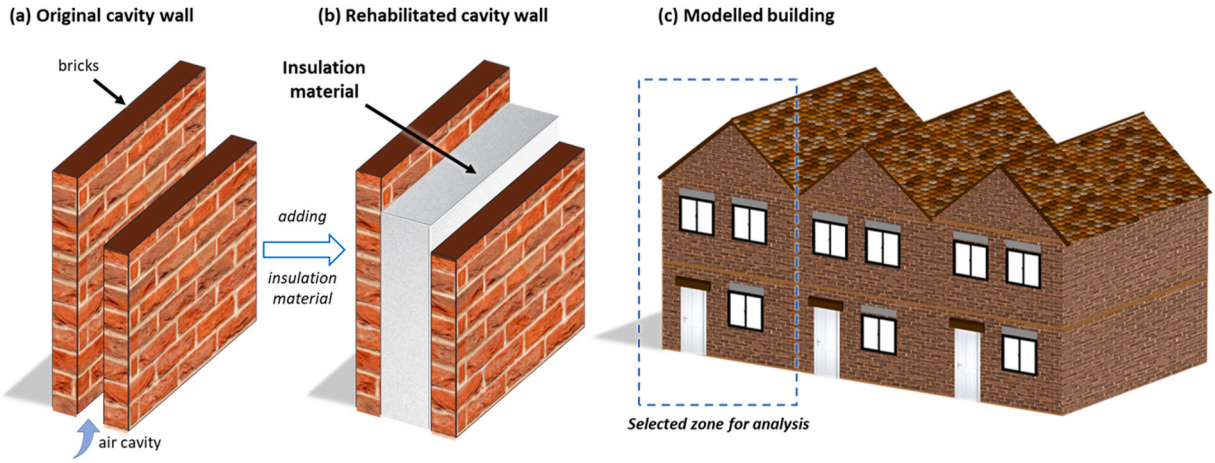

Fig. 4. (a) Simulated masonry cavity wall without and (b) with insulation material, and (c) building model for simulation.

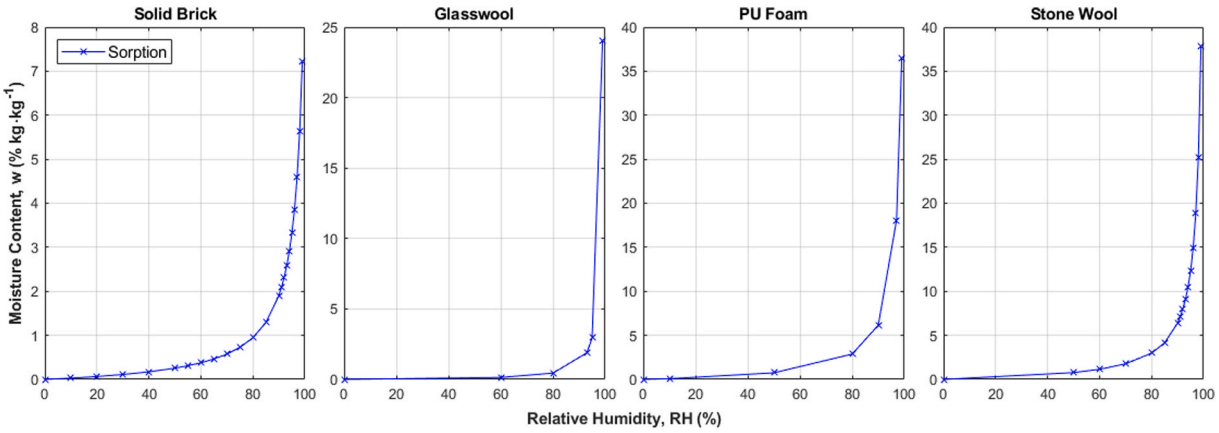

Fig. 5. Sorption curve for solid brick, glasswool, stone wool and PU foam for simulation [30]. Moisture content w after 99% RH is excluded from the plot for clarity, refer to w_{sat} for 100% relative humidity in Table 1.

Table 2
Summary of weather profile for simulated exterior climate.

Climate profile (Köppen climate classification)	Cfb
Location	Eindhoven, NLD
Altitude (m)	22
Temperature, mean (°C)	10.9
Relative humidity, mean (%)	79.5
Wind speed, mean (m·s^{-1})	3.8
Normal rain, sum (mm·a^{-1})	733.7
Counter radiation, sum (kWh·m^{-2}·a^{-1})	2883.8

and

$$\frac{\partial C}{\partial t} = \sum_j \dot{W}_{comp,j} + \dot{W}_{in} + \dot{W}_{vent} + \dot{W}_{HVAC} \tag{7}$$

respectively, where H (J) is the overall enthalpy of the air in the simulated zone, C (kg) the overall moisture content of the air in the simulated zone, $Q_{comp,j}$ (W) the transmission heat flow over component j, Q_{sol} (W) the short-wave solar radiation leading directly to heating the inner air, Q_{in} (W) the convective heat sources in the room, Q_{vent} (W) the heat flow from ventilation, Q_{HVAC} (W) the convective heat flow from building ventilation systems, $\dot{W}_{comp,j}$ (kg·s^{-1}) the moisture flow between inner wall surface j and room air, $\dot{W}_{in}$ (kg·s^{-1}) the moisture source in the room, $\dot{W}_{vent}$ (kg·s^{-1}) the moisture flow due to ventilation, and $\dot{W}_{HVAC}$ (kg·s^{-1}) the moisture flow due to building ventilation systems.

A terraced housing commonly found in the Netherlands [32] is modelled, for simplification reasons the design consists of only three small housing units (Fig. 4c), and the simulation result of the corner unit is selected for analysis. The building model has dimensions of 5 m × 8 m x 2.8 m per floor (W x D x H) per housing unit, each with a heated floor area of 80 m^2 and an unheated attic. Five different cases of masonry walls with a 6 cm cavity are included in the simulation, i.e. four different insulation materials (aerogel composite, glasswool, stone wool, PU foam) and original construction without insulation material. Other main building components that are modelled consist of ground floor assembly with U-value at 0.0956 W·m^{-2}·K^{-1}, roof assembly at 0.0867 W·m^{-2}·K^{-1}, and glazing at 0.8 W·m^{-2}·K^{-1}.

The Standard EN 16798–1 [33] is used to set the indoor environment parameters accordingly to achieve a medium level of indoor environmental quality category II (IEQ_{II}), which is related to a normal level of expectations for occupants. A heating and cooling system is included in the model to maintain an indoor temperature between 20 °C and 26 °C, and a constant air volume mechanical ventilation system to provide a steady airflow of 7 l·s^{-1} per person. The indoor heat and moisture loads are based on the software's predefined four-person family household occupancy. No mechanical humidification and dehumidification are included to limit the indoor RH level in this study. And for simplification, no natural ventilation is considered to regulate the indoor environment. The simulation is run for ten years, and the indoor temperature and RH are extracted for analysis. Two thermal comfort indices as defined by ISO 7730 [34] are assessed: the predicted mean vote (PMV) index based on a seven-point thermal sensation scale of an occupant, with a scale ranging between cold (−3) and hot (+3); and the predicted percentage dissatisfied (PPD) index which predicts the percentage of thermally dissatisfied occupants, with a value from 0% (thermally satisfied) to 100% (dissatisfied).

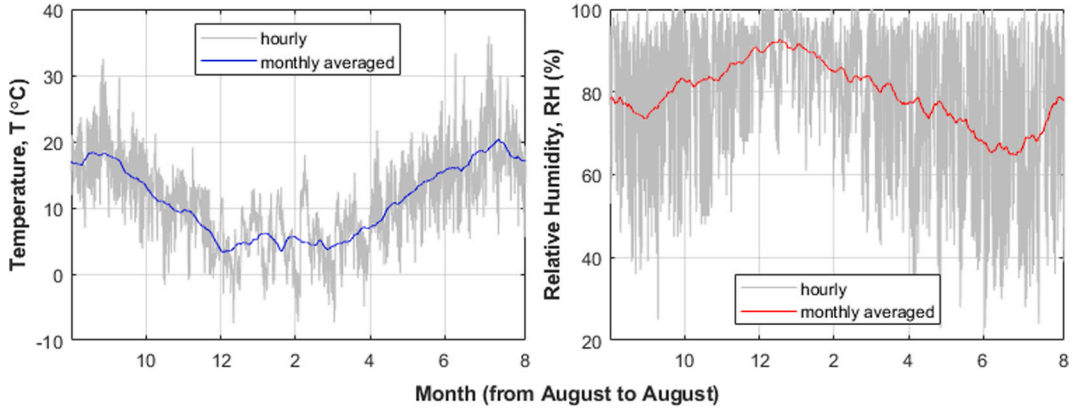

Fig. 6. Simulated Climate with Temperature and Relative Humidity profiles plotted against Months.

3. Results and discussion

3.1. Material properties

The aerogel composite has a bulk density of 88.6 $kg{\cdot}m^{-3}$ and porosity of 93.4% (Table 3) in dry conditions. The specimen maintains its form under room temperature, however, is brittle and can easily be broken into pieces by hand (Fig. 2b). Nonetheless, its mechanical strength is of no concern considering that it is protected within the cavity walls in actual application.

The aerogel composite shows low water vapour sorption properties up to 95% RH. Fig. 7 illustrates the sorption isotherm of the aerogel composite and the period for the specimen to achieve mass equilibrium ($dw/dt = 0.01\%kg{\cdot}kg^{-1}{\cdot}min^{-1}$) under the targeted RH. The equilibrium moisture content under the desorption process is only slightly higher than the adsorption process, and no significant variation between both curves is observed. Under the full immersion test, the aerogel composite however can absorb more than four times its weight of water (Table 3). The existence of binder and other additives make the aerogel composite less hydrophobic compared to pure silica aerogel. This water absorption is unproblematic however because it will be protected within the cavity wall on both sides and any direct water exposure is subsequently avoided. The specimen shows a low water vapour resistance factor at 3 under both wet and dry cup methods (Table 3).

The aerogel composite has a specific heat capacity c_p of 1273 $J{\cdot}kg^{-1}{\cdot}{^\circ}C^{-1}$ as shown in Fig. 8. This higher heat capacity is mainly attributed to its organic binder component. The specimen achieve dry thermal conductivity at 22.5 ± 0.7 $mW{\cdot}m^{-1}{\cdot}K^{-1}$ (Fig. 9) under room temperature, which is 7% higher than its main silica aerogel granulates component at 21.1 ± 0.6 $mW{\cdot}m^{-1}{\cdot}K^{-1}$. Under higher RH, the thermal conductivities increase to 22.9 ± 0.7 $mW{\cdot}m^{-1}{\cdot}K^{-1}$ at 59% RH and 23.1 ± 0.7 $mW{\cdot}m^{-1}{\cdot}K^{-1}$ at 75% RH. Fig. 9 summarizes the moisture-dependent thermal conductivity, showing a slight increase in thermal conductivity with higher RH, however, the trend is insignificant and falls within the measurement uncertainties. It should be noted that only three data points are measured, nonetheless, a simple linear fitting is included in this study as input for subsequent hygrothermal simulation.

Thermogravimetric analysis of the sample is shown in Fig. 10. The composite started to decompose at about 110 °C, and reached its maximum rate of weight loss at 320 °C and followed by another maximum at 500 °C. The composite end its volatile emissions at 650 °C at around 76% of the original dry weight.

3.2. Hygrothermal performance

The designed U-value for the reference masonry wall with a 6 cm air cavity is 1.53 $W{\cdot}m^{-2}{\cdot}K^{-1}$. When applying the aerogel composite as blown-in insulation material, its U-value is significantly improved and reduced to 0.32 $W{\cdot}m^{-2}{\cdot}K^{-1}$. Compared to the Dutch requirement, it can be seen that the rehabilitated wall using aerogel composite is performing well below the 0.71 $W{\cdot}m^{-2}{\cdot}K^{-1}$ limit required for wall renovation.

When compared to the conventional insulation materials (Fig. 11), PU foam (closed cell) can achieve the next lowest U-value after the aerogel composite, followed by glasswool and stone wool. All of these reference materials can fulfil the minimum U-value required for a retrofitted wall assuming a 6 cm cavity thickness. It should be noted that the aerogel composite is the only insulation material that can offer a new build equivalent thermal insulation performance for a cavity wall retrofitting if the cavity is thick enough (e.g. 10 cm) for sufficient insulation filling. The transient U-values of the retrofitted wall with aerogel composite and reference materials are summarized in Fig. 11. It can be observed that a steady trend of transient U-values is exhibited by the retrofitted wall when compared to the original wall without any insulation, regardless of the type of insulation material inside the cavity. The insulating performance of the non-insulated wall solely depends on its brick component, whose thermal conductivity deteriorated under higher RH, from 0.6 $W{\cdot}m^{-1}{\cdot}K^{-1}$ at the dry condition to 1.7 $W{\cdot}m^{-1}{\cdot}K^{-1}$ with moisture content at 12.6%$kg{\cdot}kg^{-1}$ [30], creating highly fluctuating transient U-values.

Table 3
Density, Porosity, Water Vapour Resistance Factor μ and Free Water Saturation for the aerogel composite.

	Aerogel Composite
Bulk density ρ_{bulk}, dried ($kg{\cdot}m^{-3}$)	88.6
Particle density $\rho_{partocle}$ ($kg{\cdot}m^{-3}$)	1340.7
Porosity (%)	93.4
Water vapour resistance factor μ	
- "Dry cup" condition (–)	3.4
- "Wet cup" condition (–)	3.4
Free water saturation w_{sat} (%)	428

The equilibrium moisture content in the aerogel composite and reference materials in a simulated year are shown in Fig. 12. The aerogel composite shows the highest moisture content in all the simulations, aligning with the fact that the inclusion of binder and additives in the composite has reduced its overall hydrophobic properties compared to standalone silica aerogel, nonetheless its averaged moisture content is still comparable to the PU foam and the stone wool, however higher than the glasswool. Both the moisture content of the aerogel composite and the glasswool have a higher fluctuation throughout the year, compared to PU foam and stone wool which have a narrower range. When inspecting the moisture content at the interfaced layers next to the exterior bricks and behind the interior bricks, it can be established that higher moisture content is amassed at the exterior interfaced layer. In the case of the aerogel composite and glasswool, substantially higher moisture contents are found during the winter months, which can be attributed to their greater moisture sorption properties under higher RH conditions during the winter period. All four insulation materials show a steady moisture content level at the interior interfaced layer. Fig. 13 summarizes the surface condensation risk at different interfaced zones. The interface between exterior bricks and insulation material for all rehabilitated walls shows higher condensation potential when compared to the original construction. No significant condensation risk is observed on the other interface layers, i.e. exterior bricks to outdoor climate, interior bricks to insulation material, and interior bricks to indoor climate. This observation is aligned with Maia et al. [23] where higher condensation potential is predicted for a rehabilitated wall under a colder climate, or when there are higher differences in thermal conductivities between different layers (existing bricks and new insulation materials) [35].

3.3. Occupant comfort assessment

The simulated indoor air temperature and RH are shown in Fig. 14 for five different cases of masonry walls with a 6 mm cavity. When the cavity in masonry walls is filled with insulation materials, the indoor RH of the reference building is reduced, from an average of 60% RH for the original air cavity wall to 56%, 56%, 55% and 54% RH when filled with glasswool, stone wool, PU foam and aerogel composite respectively. When comparing the indoor hourly RH with the IEQ_{II} limits (between 25% and 60% RH), 87% of the simulated hours in reference building using aerogel composite fall within the limits, followed by PU foam at 84%, glasswool at 82%, stone wool at 80%, and only 49% of the simulated hours in original construction without insulated cavity walls.

The indoor average room temperature increases from the original construction at 21 °C, to 22 °C for rehabilitated construction using either glasswool or stone wool, and 23 °C if using either PU foam or aerogel composite. This mean temperature increment is directly related to the annual heating and cooling demand of the reference building (Table 4). The annual heating demand is significantly reduced, up to 84% reduction in the case of aerogel composite, followed by PU foam at 81%, stone wool at 76% and glasswool at 72% compared to the original

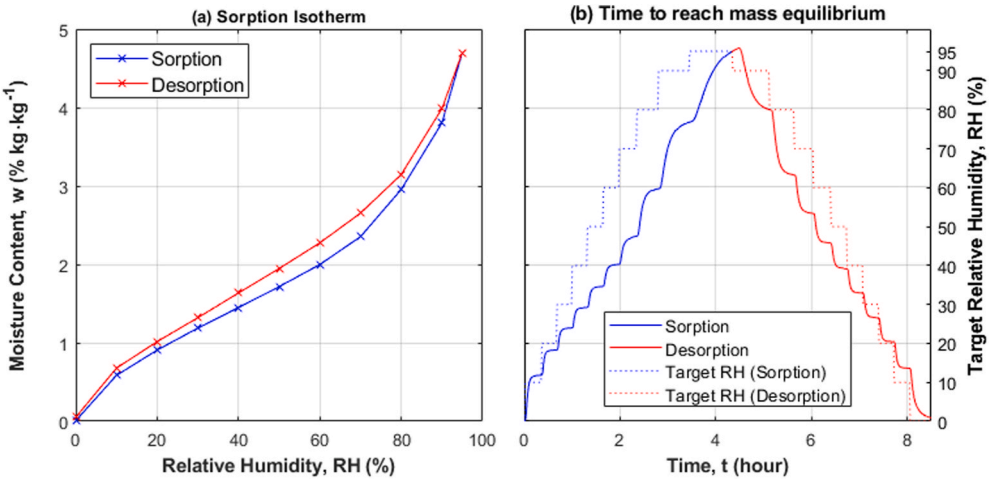

Fig. 7. (a) Sorption-desorption curves with Moisture Content w plotted against RH and (b) time to reach mass equilibrium under dw/dt = 0.01 for the aerogel composite.

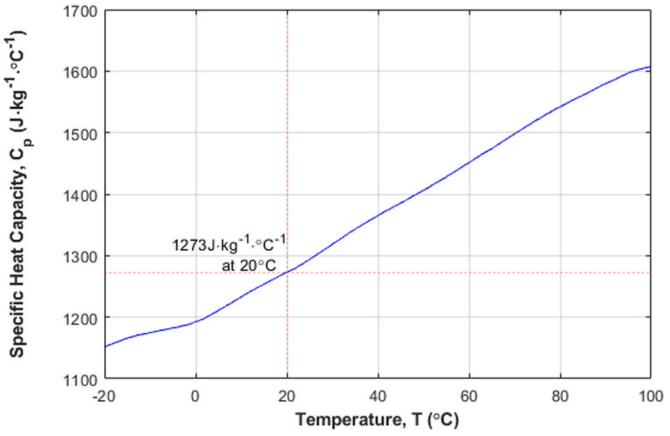

Fig. 8. Specific Heat Capacity C_p against Temperature T for the aerogel composite. C_p value at 20 °C is taken for subsequent hygrothermal study.

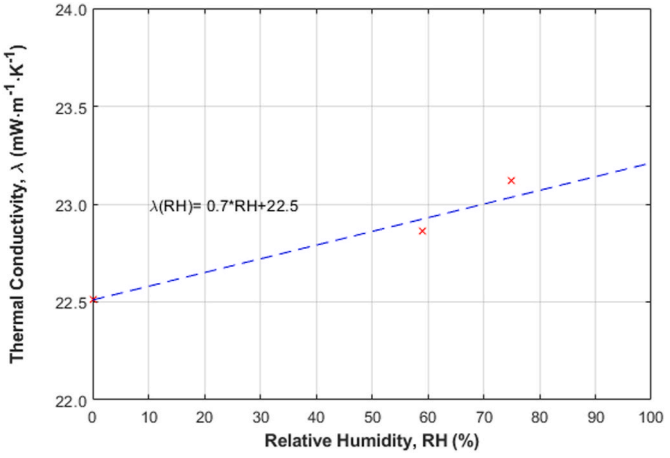

Fig. 9. Thermal Conductivity λ against RH for the aerogel composite.

construction. On the other hand, the annual cooling demand increases two to threefold. Nonetheless, the overall annual energy demand related to heating and cooling is still notably lower, with up to 72% reduction for the rehabilitated construction using aerogel composite. Note that there is no natural ventilation (through openings) to regulate the indoor

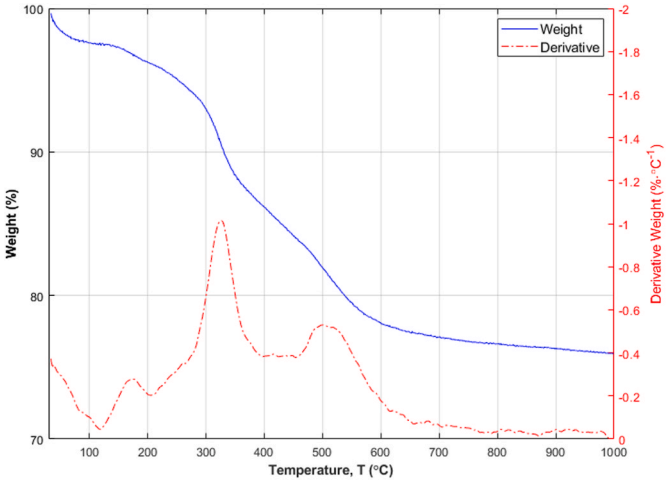

Fig. 10. Thermal stability against temperature T for the aerogel composite.

environment in this model, which could be used to substitute for the cooling demand of the rehabilitated building during the summer period.

The predicted mean vote (PMV) index and the predicted percentage dissatisfied (PPD) index of the reference buildings are shown in Fig. 15, with IEQ_{II}, IEQ_{III} and IEQ_{IV} representing medium, moderate and low expectations respectively for the indoor environmental quality from occupants. The median PMV improves from −1.5 (cool) of the original construction to −0.8 (slight cool) of rehabilitated walls with aerogel composite, corresponding to the mean PPD of 51% and 18% of thermally dissatisfied occupants respectively. While none of the rehabilitated buildings can reach a median PPD under either IEQ_{II} or IEQ_{III} due to the limited cavity thickness for applying insulation material inside, the rehabilitated buildings in all cases provide better thermal comfort than the original construction, with median PPD falling within the IEQ_{IV} limit. Notes that a lower PPD does not equal to increase in health risk but only a decrease in comfort level. The simulation results also agree with Ganobjak et al. [9], where case studies using different aerogel composites for building rehabilitation show an improvement in occupant thermal comfort.

4. Conclusions

This research examines the thermal and hygric characteristics of an advanced aerogel composite for cavity wall retrofitting and simulates its

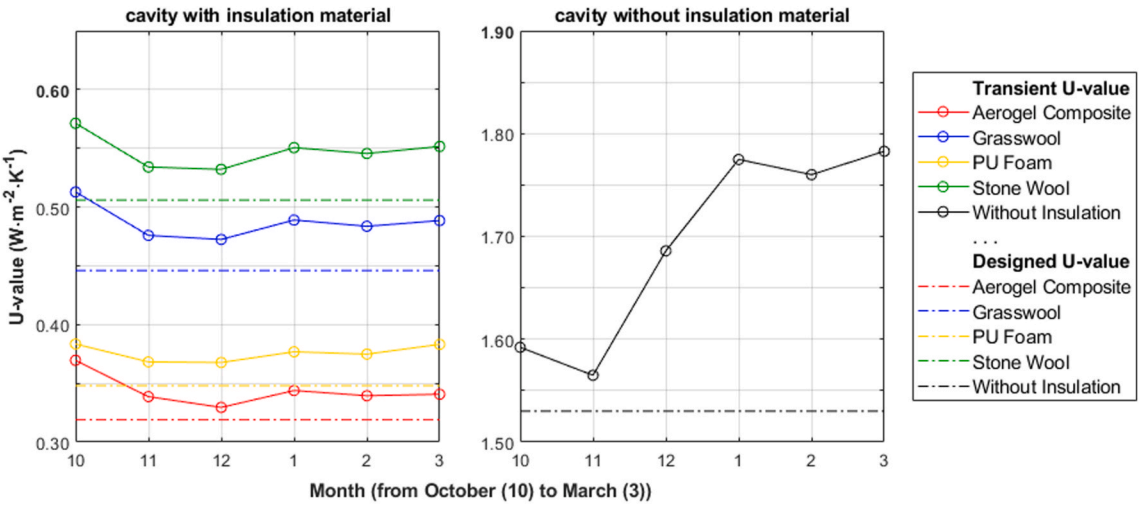

Fig. 11. Transient Thermal Transmittance (U-Value) for the masonry wall with aerogel composite, reference materials and original construction in the heating period (October to March).

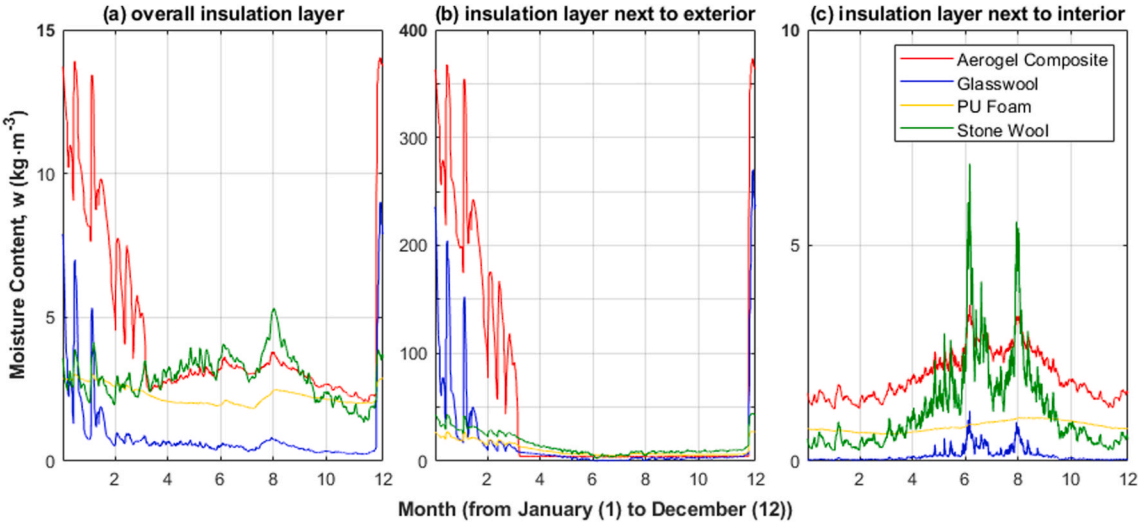

Fig. 12. Moisture Content w for the aerogel composite and reference materials in a masonry wall with 6 cm cavity thickness, showing (a) overall insulation layer, (b) at insulation layer next to the exterior and (c) next to the interior.

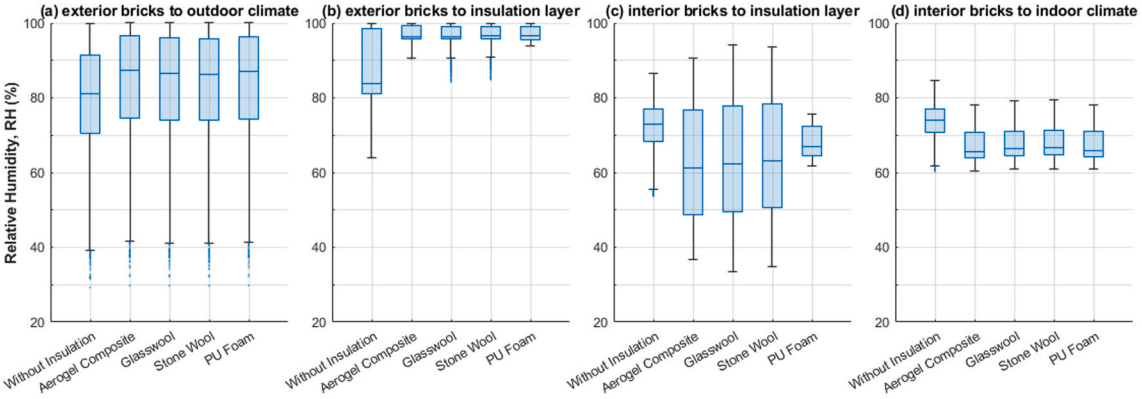

Fig. 13. Relative humidity of the (a) exterior bricks interface to outdoor climate, (b) exterior bricks interface to insulation layer, (c) interior bricks interface to insulation layer, (d) interior bricks interface to indoor climate.

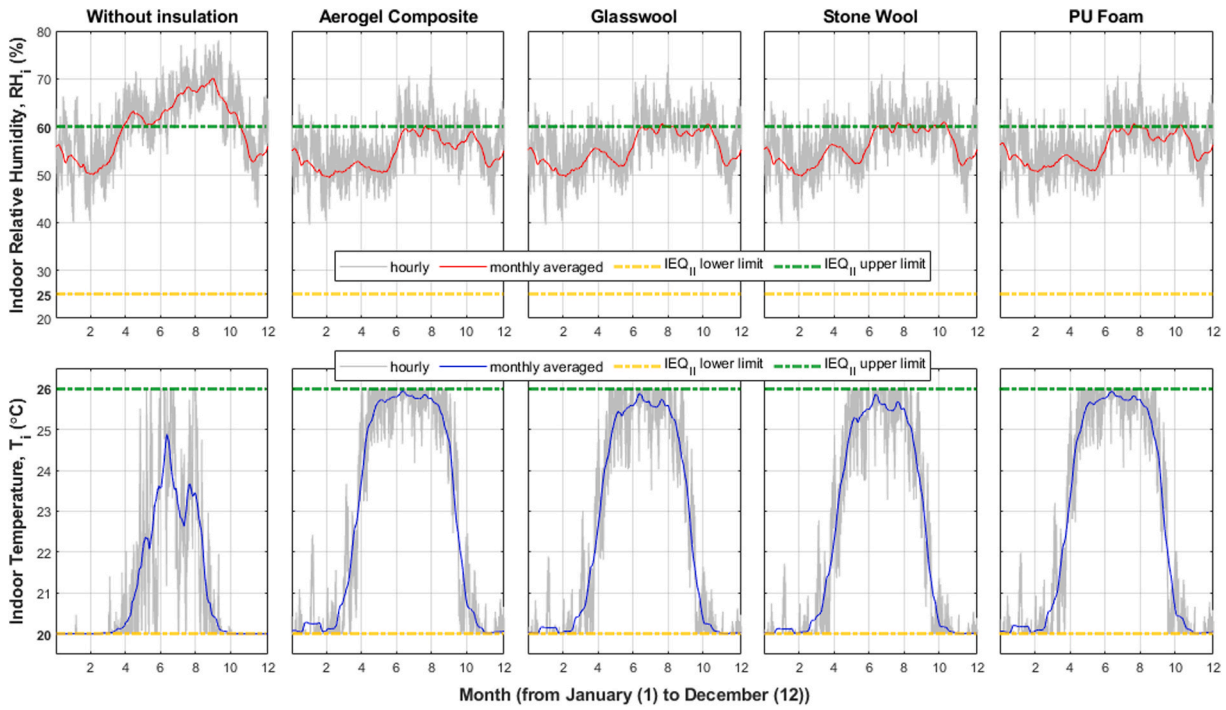

Fig. 14. Indoor Relative Humidity RH_i and Temperature T_i for the simulated building with masonry walls using aerogel composite, reference materials and original construction.

Table 4
Annual heating and cooling demand per heated area for the reference building.

Masonry wall with 6 cm cavity	Annual heating/cooling demand (kWh·m^{-2})
Without insulation	260/8
With aerogel composite	43/33
With glasswool	72/22
With stone wool	63/25
With PU foam	49/29

hygrothermal performances with typical construction details of Dutch buildings that have a cavity wall that can be filled in with insulation material. Occupant thermal comfort level is included to study the ergonomics of the thermal environment of the retrofitted reference building. Three conventional insulation materials, i.e. closed-cell PU foam, stone wool and glasswool are included in the hygrothermal and thermal comfort assessment for comparison purposes.

The aerogel composite has a notable low dry thermal conductivity of 22.5 mW·m^{-1}·K^{-1} at 20 °C, only 7% higher than pure silica aerogel granulates, and shows a slight increase in thermal conductivity with higher RH. The composite exhibits thermal stability up to 110 °C before starting to decompose. The composite also shows low water vapour sorption properties, attributed to the hydrophobic characteristics of its main silica aerogel component. It has a low density of 88.6 kg·m^{-3} and porosity of 93.4%, with a low water vapour resistance factor of 3.

The designed U-value for a retrofitted masonry wall with a 6 cm cavity using the aerogel composite is at 0.32 W·m^{-2}·K^{-1}, which is significantly below the 0.71 W·m^{-2}·K^{-1} limit for a renovated wall under Dutch requirements. The aerogel composite however exhibits higher fluctuation of moisture content during the winter months at its interface

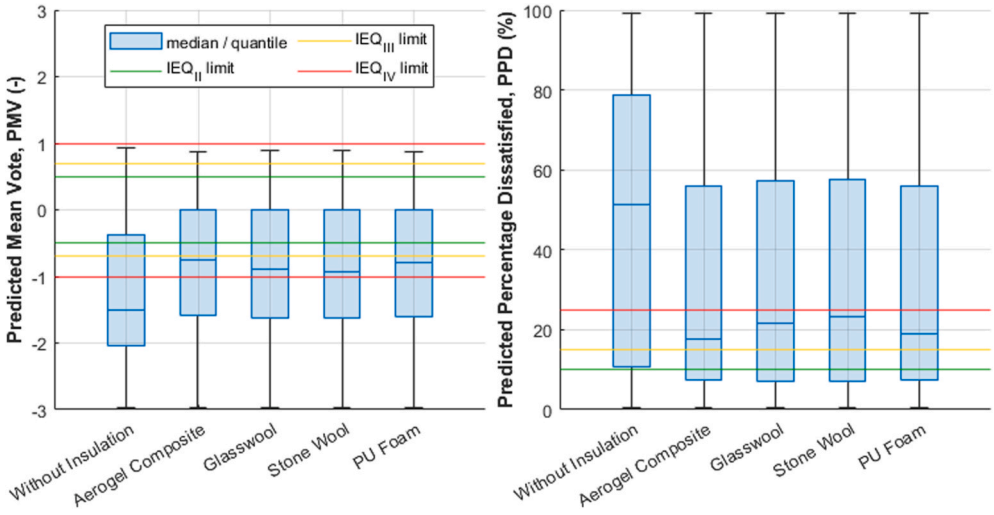

Fig. 15. Predicted Mean Vote PMV and Predicted Percentage Dissatisfied PPD for the simulated building with masonry walls using aerogel composite, reference materials and original construction.

layer next to the exterior bricklayer, attributed to its greater moisture sorption properties under high RH conditions during the winter period in the Netherlands.

When the cavity in masonry walls is filled with the aerogel composite, the indoor RH of the reference building is reduced, from an average of 60% RH for the original air cavity wall to 54% RH. This is equivalent to 87% of the simulated hours being within the IEQ_{II} limits for a rehabilitated building using aerogel composite, compared to only 49% in original construction without insulated cavity walls. The annual heating and cooling demand are significantly reduced, up to 72% reduction compared to the original construction.

The median PMV improves from −1.5 (cool) of the original construction to −0.8 (slightly cool) of rehabilitated walls with aerogel composite, corresponding to the mean PPD of 51% and 18% of thermally dissatisfied occupants respectively. The rehabilitated buildings in all cases (aerogel composite, glasswool, stone wool, PU foam) provide better thermal comfort than the original construction, with median PPD falling within the IEQ_{IV} limit.

This article features the suitability of using the tested aerogel composite for cavity wall retrofitting purposes under the Netherlands climate, which can outperform conventional insulation materials in the market, without requiring major renovation and sacrificing the thermal comfort of its occupants.

In order to validate the results of this study, it will be necessary to carry out an in-field monitoring and survey campaign.

CRediT authorship contribution statement

C.H. Koh: Writing – original draft, Software, Methodology, Investigation, Formal analysis, Conceptualization. **K. Schollbach:** Writing – review & editing, Supervision. **F. Gauvin:** Writing – review & editing, Supervision. **H.J.H. Brouwers:** Writing – review & editing, Supervision, Funding acquisition.

Declaration of competing interest

The authors declare the following financial interests/personal relationships which may be considered as potential competing interests: C. H. Koh reports financial support was provided by project BRIMM (Bright Renovatie Isolatie voor woningschil door (Advanced) Materialen en Methodes) under Missiegedreven Onderzoek, Ontwikkeling en Innovatie (MOOI).

Data availability

Data will be made available on request.

Acknowledgements

This research is funded by project BRIMM (Bright Renovatie Isolatie voor woningschil door (Advanced) Materialen en Methodes) under Missiegedreven Onderzoek, Ontwikkeling en Innovatie (MOOI).

References

[1] Rijksdienst voor Ondernemend Nederland, Monitor Energiebesparing Gebouwde Omgeving, Monitor Energy Saving Built Environment), Utrecht, 2021.
[2] Rijksoverheid, Klimaatakkoord (Climate Agreement), Den Haag, 2019.
[3] Rijksdienst voor Ondernemend Nederland, Lange Termijn Renovatiestrategie: Op Weg Naar Een CO2-arme Gebouwde Omgeving (Long-Term Renovation Strategy: En Route to a low-CO2 Built Environment), Den Haag, 2020.
[4] Rijksdienst voor Ondernemend Nederland, Marktinformatie isolatiematerialen, isolatieglas en HR-ketels 2010-2020 (Market information on insulation materials, insulating glass and high-efficiency boilers 2010-2020), Den Haag, 2021.
[5] Spouwmuurisolatie (Cavity Wall Insulation), Milieu Centraal, 2022 [Online]. Available: https://www.milieucentraal.nl/energie-besparen/isoleren-en-besparen/spouwmuurisolatie/. (Accessed 31 March 2022).
[6] Bouwbesluit, Artikel 5.6 Verbouw (Renovation), 2012.
[7] Bouwbesluit, Artikel 5.3 Thermische Isolatie (Thermal Insulation), 2012.
[8] M.M. Koebel, J. Wernery, W.J. Malfait, Energy in buildings - policy, materials and solutions, MRS Energy Sustain.: A Rev. J. 4 (2017) e12, https://doi.org/10.1557/mre.2017.14.
[9] M. Ganobjak, S. Brunner, J. Wernery, Aerogel materials for heritage buildings: materials, properties and case studies, J. Cult. Herit. (42) (2020) 81–98, https://doi.org/10.1016/j.culher.2019.09.007.
[10] I. Rodríguez-Maribona, Final Report Summary - Effesus (Energy Efficiency for EU Historic Districts Sustainability), 2017 [Online]. Available: https://cordis.europa.eu/project/id/314678/reporting.
[11] E. Lucchi, F. Roberti, T. Alexandra, Definition of an experimental procedure with the hot box method for the thermal performance evaluation of inhomogeneous walls, Energy Build. 179 (2018) 99–111, https://doi.org/10.1016/j.enbuild.2018.08.049.
[12] E. Lucchi, F. Becherini, M.C. Di Tuccio, A. Troi, J. Frick, F. Roberti, C. Hermann, I. Fairnington, G. Mezzasalma, L. Pockelé, A. Bernardi, Thermal performance evaluation and comfort assessment of advanced aerogel as blown-in insulation for historic buildings, Build. Environ. 122 (2017) 258–268, https://doi.org/10.1016/j.buildenv.2017.06.019.
[13] Sprayable Aerogel Bead Compositions with High Shear Flow Resistance and High Thermal Insulation Value, NASA Tech Briefs, 2022 [Online]. Available: https://ntrs.nasa.gov/citations/20130012683. (Accessed 21 April 2022).
[14] Silfoam, Active Aerogels, 2022 [Online]. Available: https://www.activeaerogels.com/spray-on/. (Accessed 21 April 2022).
[15] E. Cuce, P.M. Cuce, C.J. Wood, S.B. Riffat, Toward aerogel based thermal superinsulation in buildings: a comprehensive review, Renew. Sustain. Energy Rev. 34 (2014) 273–299, https://doi.org/10.1016/j.rser.2014.03.017.
[16] B. Chal, G. Foray, B. Yrieix, K. Masenelli-Varlot, L. Roiban, J.M. Chenal, Durability of silica aerogels dedicated to superinsulation measured under hygrothermal conditions, Microporous Mesoporous Mater. 272 (2018) 61–69, https://doi.org/10.1016/j.micromeso.2018.05.047.
[17] K. Nocentini, P. Achard, P. Biwole, Hygro-thermal properties of silica aerogel blankets dried using microwave heating for building thermal insulation, Energy Build. 158 (2018) 14–22, https://doi.org/10.1016/j.enbuild.2017.10.024.
[18] M. Ibrahim, K. Nocentini, M. Stipetic, S. Dantz, F.G. Caiazzo, H. Sayegh, L. Bianco, Multi-field and multi-scale characterization of novel super insulating panels/systems based on silica aerogels: thermal, hydric, mechanical, acoustic, and fire performance, Build. Environ. 151 (2019) 30–42, https://doi.org/10.1016/j.buildenv.2019.01.019.
[19] H. Guo, S. Cai, K. Li, Z. Liu, L. Xia, J. Xiong, Simultaneous test and visual identification of heat and moisture transport in several types of thermal insulation, Energy 197 (2020), 117137, https://doi.org/10.1016/j.energy.2020.117137.
[20] Y. Liu, H. Wu, Y. Zhang, J. Yang, F. He, Structure characteristics and hygrothermal performance of silica aerogel composites for building thermal insulation in humid areas, Energy Build. 228 (2020), 110452, https://doi.org/10.1016/j.enbuild.2020.110452.
[21] N. Sakiyama, J. Frick, M. Stipetic, T. Oertel, H. Garrecht, Hygrothermal performance of a new aerogel-based insulating render through weathering: impact on building energy efficiency, Build. Environ. 202 (2021), 108004, https://doi.org/10.1016/j.buildenv.2021.108004.
[22] S. Fantucci, E. Fenoglio, G. Grosso, V. Serra, M. Perino, V. Marino, M. Dutto, Development of an aerogel-based thermal coating for the energy retrofit and the prevention of condensation risk in existing buildings, Sci. Technol. Built Environ. 25 (9) (2019) 1178–1186, https://doi.org/10.1080/23744731.2019.1634931.
[23] J. Maia, M. Pedroso, N. Ramos, P. Pereira, I. Flores-Colen, M.G. Gomes, L. Silva, Hygrothermal performance of a new thermal aerogel-based render under distinct climatic conditions, Energy Build. 243 (2021), 111001, https://doi.org/10.1016/j.enbuild.2021.111001.
[24] ASTM, "ASTM C1498-01 Standard Test Method for Hygroscopic Sorption Isotherms of Building Materials".
[25] ASTM, "ASTM E96-00 Standard Test Methods for Water Vapour Transmission of Materials".
[26] WUFI, WUFI Pro 6.4 Online Help, Appendix: Basic: Moisture Transport in Building Materials.
[27] M. Salonvarra, A. Karagiozis, M. Pazera, W. Miller, Air Cavities behind Claddings - what Have We Learned?, 1995.
[28] D. Crawley, L. Lawrie, Climate.OneBuilding.Org [Online]. Available: https://climate.onebuilding.org/default.html. (Accessed 25 March 2022).
[29] ISO, ISO 13788 Hygrothermal Performance of Building Components and Building Elements - Internal Surface Temperature to Avoid Critical Surface Humidity and Interstitial Condensation - Calculation Method, 2012.
[30] WUFI, WUFI Material Database, 2022.
[31] WUFI, WUFI Plus 3.1 Manual.
[32] CBS, Vier op de tien huishoudens wonen in een rijtjeshuis (Four in ten households live in a terraced house) [Online]. Available: https://www.cbs.nl/nl-nl/nieuws/2016/14/vier-op-de-tien-huishoudens-wonen-in-een-rijtjeshuis. (Accessed 2 May 2022).
[33] CEN, EN 16798-1 Energy Performance of Buildings - Ventilation for Buildings - Part 1: Indoor Environmental Input Parameters for Design and Assessment of Energy Performance of Buildings Addressing Indoor Air Quality, Thermal Environment, lighting and acoustics, 2019.
[34] ISO, ISO 7730 Ergonomics of the Thermal Environment - Analytical Determination and Interpretation of Thermal Comfort Using Calculation of the PMV and PPD Indices and Local Thermal Comfort Criteria, 2005.
[35] P. Moradias, P.D. Silva, J. Castro-Gomes, M. Salazar, L. Pires, Experimental study on hygrothermal behaviour of retrofit solutions applied to old building walls, Construct. Build. Mater. 35 (2012) 864–873, https://doi.org/10.1016/j.conbuildmat.2012.04.138.